Jurnal Teknik Informatika (JUTIF) Vol. 7, No. 3, June 2026, Page. 2131-2153
P-ISSN: 2723-3863 https://jutif.if.unsoed.ac.id
E-ISSN: 2723-3871 DOI: https://doi.org/10.52436/1.jutif.2026.7.3.5436

Integrating Whale Transaction Flow Scoring with LSTM for Bitcoin Trend Forecasting

Muhammad Ridhwan Hakiki*[1], Kusnawi[2]

[1,2]Informatics, Universitas Amikom Yogyakarta, Indonesia

Email: [1]hakikimuhammad@students.amikom.ac.id

Received : Nov 10, 2025; Revised : Dec 16, 2025; Accepted : Dec 21, 2025; Published : Jun 15, 2026

Abstract

Bitcoin price prediction faces significant challenges due to high volatility and the influence of large holders, known as whales, whose transactions exceeding 500 BTC can affect market behavior. This study develops an LSTM model combining whale transaction sentiment scores with historical Bitcoin OHLC prices to forecast 7-day ahead price movements. The dataset comprises 2,069 whale transactions and 8,761 hourly price observations from April 20, 2024 to April 20, 2025. The scoring mechanism assigns +1 to exchange outflows, -1 to inflows, and 0 to neutral transfers, multiplied by logarithmically normalized transaction amounts. The LSTM architecture consists of two recurrent layers with 128 and 64 memory units, processing 720-hour input sequences to generate 168-hour OHLC forecasts. Training evaluation yielded R^2 of 0.9386, RMSE of 0.0686, and MAE of 0.0498. Test evaluation produced Mean Absolute Errors ranging from 871.72 USD to 3,482.27 USD across OHLC components. The model correctly predicted upward directional trends but systematically underestimated prices by 2,000-3,000 USD initially and failed to anticipate a 6,422 USD intraday surge on April 22, 2025. Results demonstrate that whale sentiment features enhance directional trend identification but do not enable precise multi-day price point prediction due to sudden market regime changes. These findings contribute empirical evidence that directional sentiment scoring of large-holder transactions provides complementary predictive value beyond conventional price-volume indicators, establishing a methodological foundation for integrating blockchain-native behavioral signals into cryptocurrency forecasting frameworks.

Keywords : *Bitcoin, Cryptocurrency, Forecasting, LSTM, Sentiment analysis, Whale transactions*

1. INTRODUCTION

Bitcoin was first introduced as a decentralized peer-to-peer electronic cash system by Nakamoto in 2008, utilizing a distributed proof-of-work network to validate and timestamp transactions, enabling secure digital payments without intermediaries [1]. Over the years, Bitcoin has evolved beyond its initial purpose as an alternative payment method into a speculative investment asset, attracting both retail and institutional investors worldwide, with its unique characteristics, including decentralization, transparency, and a fixed supply contributing to its significant price volatility [2].

Bitcoin exhibits substantially higher volatility compared to traditional assets, with the standard deviation of Bitcoin's daily return rate reaching 3.85% during the seven-year period from April 2015 to April 2022, representing 2.68 times the standard deviation of gold's return rate and 3.36 times that of the S&P500 during the same period [3]. This extreme volatility has attracted growing interest among experts, as economists suppose that Bitcoin and its fundamentals differ from those of conventional assets such as stocks, bonds, or foreign exchanges because Bitcoin is not a corporation [2]. Due to these large price fluctuations, both the function of Bitcoin as a store of value as a commodity and its transaction payment function as a currency have been questioned [4]. Counterintuitively, investors in cryptoassets face high risk when holding for longer periods and might be interested in diversifying outside of cryptoassets, as they tend to move together considerably during extreme events and swings in both directions [5].

The decentralized infrastructure and high-risk profile of the Bitcoin market can yield speculative opportunities and market inefficiencies [6]. One major difference between Bitcoin and traditional stocks is that while stocks trade only at certain times on weekdays, the Bitcoin market typically operates around the clock, allowing investors to buy or sell Bitcoin all day, which may result in Bitcoin price fluctuations at unpredictable times [7]. Research on explanatory variables for Bitcoin price movements reveals nuanced relationships: trading volume and Google trends are all insignificant in both univariate and multivariate regressions, while the unique address variable is significant in univariate regression but not in multivariate regression, potentially due to its correlation with transaction volume; however, transaction volume itself remains significant in both regression types [8].

Crypto whales exert considerable influence on the cryptocurrency market through their substantial holdings and trading activities, affecting crypto market liquidity and increasing price volatility through changes in the supply of cryptoassets. Because whales often hold their cryptocurrencies for extended periods without any transactions, they create a shortage of supply in circulation; additionally, they may cause large price movements when they suddenly become active and start adding large volumes of cryptocurrencies into circulation [9]. Moreover, empirical evidence indicates that such market dynamics are often driven by concentrated capital holders exercising strategic influence. Research identifies that specific large-scale trading activities—attributable to single large entities—are often timed to follow market downturns, effectively inducing sizable price appreciations. These patterns support the view that sophisticated market participants leverage their significant capital to exert an extremely large price impact, thereby capturing substantial gains during periods of high speculation [10].

In order to make investment decisions in the crypto market, it is necessary to have efficient tools for price forecasting, profitability, and risk assessment, at least for the short-term time horizon [11]. Machine learning techniques, particularly deep learning models, have emerged as promising approaches for Bitcoin price prediction. Long Short-Term Memory (LSTM) networks have demonstrated effectiveness in cryptocurrency price forecasting, as with the utilization of gates in each cell, data can be filtered, discarded, or added, enabling LSTM networks to identify both short and long-term correlation features within time series [12]. Utilizing historical Bitcoin price data from 2014 to 2023, extensive evaluations indicate that LSTM models provide highly accurate predictions, with a Mean Squared Error (MSE) of 0.0001798 and a Mean Absolute Error (MAE) of 0.0101322, demonstrating that LSTM effectively captures the complex and dynamic patterns of Bitcoin prices, outperforming other methods [13]. However, the selection of explanatory variables requires careful consideration, as using too few explanatory variables reduces prediction accuracy; for example, adding additional variables to a lightweight model with four bitcoin price OHLC variables improves prediction accuracy [3].

Comparative analysis of neural network architectures reveals varying levels of performance in Bitcoin price prediction. The BP neural network showed MAE of 416.09, RMSE of 515.35, and MAPE of 2.85%, with precision of 0.59, recall of 0.58, and F1 score of 0.55; CNN models achieved superior performance with MAE of 215.98, RMSE of 261.90, and MAPE of 2.03%, along with precision of 0.64, recall of 0.63, and F1 score of 0.60; while LSTM models yielded MAE of 229.78, RMSE of 297.97, and MAPE of 2.75%, with precision of 0.58, recall of 0.73, and F1 score of 0.63 [14]. These findings suggest that hybrid CNN-LSTM models and standalone CNN architectures demonstrate considerable promise for capturing the complex dynamics of Bitcoin prices, though the 24/7 nature of cryptocurrency markets, the influence of large holders, and the multifaceted nature of price determinants present ongoing challenges for accurate prediction and risk management.

Jurnal Teknik Informatika (JUTIF) Vol. 7, No. 3, June 2026, Page. 2131-2153
P-ISSN: 2723-3863 https://jutif.if.unsoed.ac.id
E-ISSN: 2723-3871 DOI: https://doi.org/10.52436/1.jutif.2026.7.3.5436

Given the extensive research on Bitcoin price prediction and the effectiveness of deep learning approaches, this study develops and evaluates an LSTM-based model for 7-day-ahead forecasting that integrates OHLC data with a novel dynamic whale scoring mechanism. While previous studies have examined market reactions to large Bitcoin transfers [15], existing methodologies predominantly employ binary classification frameworks that identify whale transactions as discrete events without quantifying their directional market implications. The proposed whale scoring system advances beyond this threshold-based detection paradigm by assigning continuous positive scores to exchange outflows (signaling accumulation behaviour) and negative scores to exchange inflows (indicating distribution patterns), with scoring magnitudes calibrated proportionally to transaction size relative to market liquidity. This directional weighting approach fundamentally differs from conventional volume-based whale detection methods, which treat all large transactions uniformly regardless of their underlying market intent or potential price impact. Furthermore, whereas existing LSTM-based forecasting models predominantly rely on technical indicators and price data alone, the integration of continuous, direction-aware whale activity metrics as exogenous predictive features remains underexplored in medium-term Bitcoin price forecasting literature. The analysis covers the one-year period from April 20, 2024, to April 20, 2025, immediately following the Bitcoin halving event, and empirically investigates whether directionally-weighted whale transaction data enhance LSTM forecast accuracy beyond conventional feature sets for weekly price prediction.

2. METHOD

This study introduces a methodological framework for Bitcoin trend prediction, which combines whale transaction flow scoring with a Long Short-Term Memory (LSTM) network.

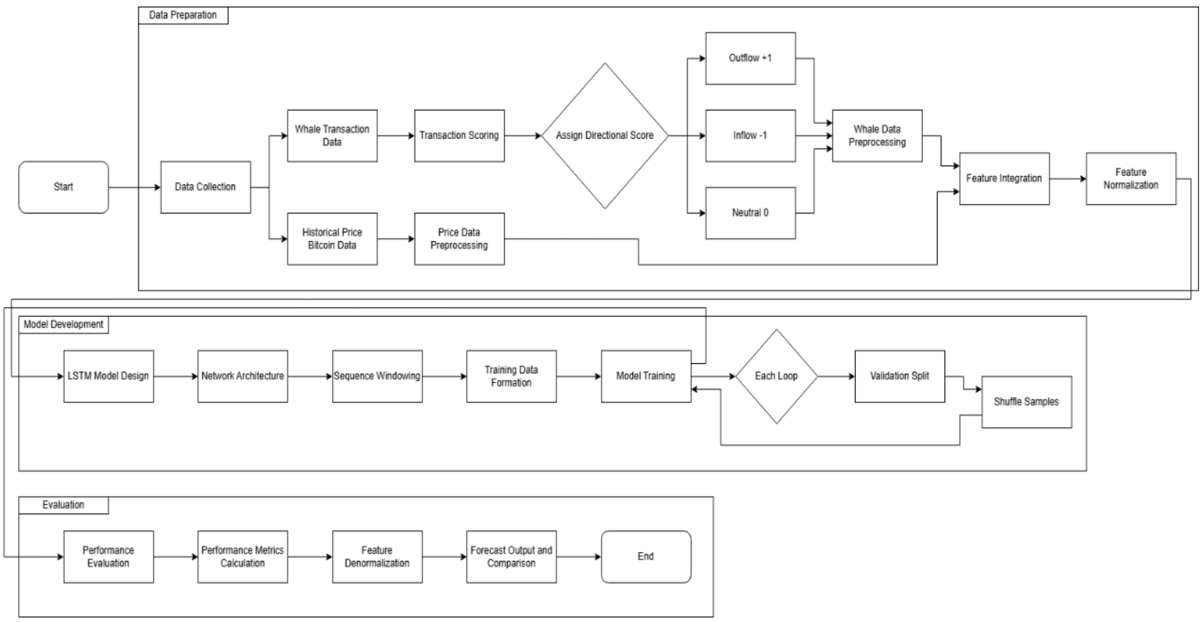

Figure 1. Research Methodology: LSTM-Based Bitcoin Forecasting with Whale Data

As visualized in Figure 1, the proposed approach comprises three sequential stages. The Data Preparation stage focuses on acquiring and processing the necessary datasets. This is followed by the Model Development stage, where the LSTM network is designed and trained. Finally, the Evaluation stage assesses the model's forecasting accuracy. Each stage is detailed in the subsequent sections.

2.1. Data Collection

2.1.1. Whale Transaction

Whale transaction data were obtained from the Whale Alert API for the corresponding temporal period, capturing large-scale Bitcoin transfers with transaction amounts equal to or greater than 500 BTC [15]. Each transaction record contains the timestamp (*created_at_utc*), source address (*from_entity*), destination address (*to_entity*), and the transferred amount in Bitcoin. Transactions were systematically classified based on entity involvement. Exchanges were defined as major centralized cryptocurrency trading platforms, including Binance, Bitfinex, Bitstamp, Coinbase, and Kraken, as well as other prominent exchanges such as Bybit, Huobi, Gemini, BitGet, Bitmex, Bittrex, Gate.io, KuCoin, and Coincheck [16][17][18]. All entities not identified as exchanges were categorized as "unknown," which encompasses institutional wallets, private addresses, and unidentified entities.

2.1.2. Historical Bitcoin Price

Historical Bitcoin price data in USD were obtained from CoinDesk, spanning the period from April 20, 2024, 00:00:00 UTC to April 20, 2025, 00:00:00 UTC. The dataset comprises hourly observations of OHLC (Open, High, Low, Close) prices, which serve as the primary market indicators for price movement analysis [19]. To evaluate the model's predictive performance, a separate dataset covering the period from April 20, 2025, 00:00:00 UTC to April 27, 2025, 23:59:59 UTC was reserved. This dataset, also on an hourly OHLC basis, is used solely for forecasting validation and comparison, allowing for an assessment of model accuracy over a 7-day prediction horizon [20].

2.2. Transactions Scoring

The whale transaction scoring mechanism was developed to quantify market sentiment based on the directional flow of large Bitcoin transfers relative to centralized exchanges. The scoring system operates on the principle that transaction directionality serves as a proxy for market sentiment [15][21]. Exchange outflows, defined as fund transfers from exchange wallets to unknown entities, are assigned positive sentiment scores. This classification reflects bullish market sentiment, as Bitcoin withdrawal from trading platforms typically indicates accumulation behaviour and reduced selling pressure [22]. Conversely, exchange inflows, representing fund transfers from unknown entities to exchange wallets, receive negative sentiment scores, signifying bearish sentiment as such movements often precede liquidation or selling activities [15]. Inter-exchange transfers and transfers between unknown entities are assigned neutral scores of zero, as these transactions do not represent net capital inflows or outflows from the trading ecosystem.

To account for transaction magnitude heterogeneity, two derived features were computed. First, the *scaled_amount* was calculated through logarithmic normalization to address the wide distribution of transaction volumes [17]:

$$scaled_{amount} = \frac{\ln(1 + amount) - \ln(1 + amount_{min})}{\ln(1 + amount_{max}) - \ln(1 + amount_{min})} \tag{1}$$

where amount represents the transaction value in BTC, *amount_min* denotes the minimum transaction amount within the dataset, and *amount_max* represents the maximum transaction amount.

Second, the *sentiment_score* was derived as the product of the directional indicator and the scaled transaction amount [15]:

$$sentiment_{score} = directional_{indicator} \times scaled_{amount} \tag{2}$$

where the directional indicator assumes values of +1 for exchange outflows (bullish), −1 for exchange inflows (bearish), and 0 for neutral transfers (inter-exchange or unknown-to-unknown). After computing individual transaction scores, temporal aggregation was performed at hourly intervals. Within each one-hour window, the amount and *scaled_amount* values were summed to capture total transaction volume, and *sentiment_score* values were averaged to produce hourly sentiment indicators aligned with the Bitcoin price data.

2.3. Data Preprocessing

The preprocessing pipeline was implemented separately for the whale transaction dataset and the historical Bitcoin price dataset to ensure temporal consistency and data integrity prior to model integration [23].

2.3.1. Whale Transaction

For the whale transaction dataset, dimensionality reduction was performed by retaining only the timestamp (*created_at_utc*) and the computed *sentiment_score* variables. The dataset was indexed by timestamp and resampled to one-hour intervals using mean aggregation. This resampling operation converted transaction-level observations into hourly aggregated sentiment values.

2.3.2. Bitcoin Price

For the historical Bitcoin price dataset, hourly OHLC aggregation was performed through temporal resampling [20]. Within each one-hour window, the aggregation function selected the first value for the opening price (*open*), the maximum value for the high price (*high*), the minimum value for the low price (*low*), and the final value for the closing price (*close*).

2.3.3. Feature Integration

Following independent preprocessing, both datasets were temporally aligned and merged using the timestamp index as the join key. The resulting integrated dataset contains synchronized hourly observations comprising Bitcoin market indicators (*open*, *high*, *low*, *close*) and the corresponding whale sentiment feature (*sentiment_score*).

2.3.4. Feature Normalization

To facilitate model convergence and prevent feature dominance effects, all variables were normalized using the Min-Max scaling technique [24]. This transformation rescales all features to the standardized range [0, 1] according to the following equation:

$$Xnormalized = Xmax - XminX - Xmin \quad (3)$$

where X represents the original feature value, X_min denotes the minimum value of the feature across the dataset, and X_max represents the maximum value.

2.4. LSTM Model

2.4.1. LSTM Network Architecture

The proposed LSTM model consists of five layers, as summarized in Table 1. The first LSTM layer contains 128 memory units with *return_sequences=True*, followed by a dropout layer with a 0.2 dropout rate. The second LSTM layer has 64 memory units with *return_sequences=False*, followed by another dropout layer with a 0.2 dropout rate. The dense output layer consists of 672 neurons.

The selection of 128 and 64 memory units for the respective LSTM layers is grounded in empirical validation from prior research. Studies employing this 128-64 unit configuration have demonstrated effective modeling of financial time series, achieving Root Mean Square Error (RMSE)

Vol. 7, No. 3, June 2026, Page. 2131-2153
https://jutif.if.unsoed.ac.id
DOI: https://doi.org/10.52436/1.jutif.2026.7.3.5436

values as low as 18.89 on test data [25], thereby providing empirical justification for this architectural design choice. The complete network architecture is summarized in Table 1.

Table 1. LSTM Architecture

First LSTM Layer	**First Dropout Layer**	**Second LSTM Layer**	**Second Dropout Layer**	**Dense Output Layer**
128 memory units with return_sequences=True	0.2 dropout rate	64 memory units with return_sequences=False	0.2 dropout rate	672 neurons

2.4.2. Sequence Window

The LSTM model processes temporal data using a sliding window approach, in which each input sequence consists of 720 consecutive hourly observations, equivalent to 30 days. This window size defines the number of past hours considered for predicting future values. The selection of this 30-day window is grounded in empirical findings demonstrating that 30-day periods present the best performance with significantly lower forecast errors compared to shorter or longer durations. Research hypotheses regarding the efficiency of lookback periods confirmed that very short or very long periods tend to increase prediction error, highlighting the importance of proper window selection for LSTM models in volatile markets. Furthermore, statistical analysis has confirmed the significant influence of the lookback period on model performance [26].

The forecast horizon is set to 168 hours, corresponding to 7 days, representing the multi-step prediction target. Input features for each window include the four OHLC variables (*open*, *high*, *low*, *close*) and the *sentiment_score* derived from whale transaction data. The model is trained to produce predictions for OHLC values at each timestep within the 168-hour forecast horizon. Table 2 summarizes these parameters, including input and output features.

Table 2. Sequence Window

Parameter	**Value**	**Description**
Window size	720 hours	Input sequence length (30 days)
Forecast horizon	168 hours	Multi-step ahead prediction (7 days)
Input features	OHLC + sentiment_scores	Features used for training
Output features	OHLC	Predicted values per timestep

2.4.3. Training Data

The training dataset was generated using a sliding window approach. Each sample consists of a 720-hour input sequence with five features: open, high, low, close, and sentiment_score, and a 168-hour target sequence with four features: open, high, low, and close. The window advances one time step at a time to produce successive samples, and each target sequence is reshaped into a 672-dimensional vector.

$$\begin{gathered} X_{train}^{(i)} = data[i - 720{:}\, i], \\ y_{train}^{(i)} = reshape(data[i{:}\, i + 168, 0{:}\, 4], 168 \times 4), \\ i = 720 \dots n - 168 \end{gathered} \tag{4}$$

2.4.4. Model Compilation

The LSTM model was trained for 20 epochs with a batch size of 32 samples, as summarized in Table 3 A 10% validation split was applied, and the training samples were shuffled at each epoch.

Vol. 7, No. 3, June 2026, Page. 2131-2153
https://jutif.if.unsoed.ac.id
DOI: https://doi.org/10.52436/1.jutif.2026.7.3.5436

Table 3. Model Configuration

Epochs	Batch Size	Validation Split	Shuffle
20 iterations	32 samples	10% for monitoring overfitting	Training samples randomized each epoch

2.5. Evaluation Metrics

The LSTM model's performance was evaluated using MSE, RMSE, MAE, and R^2 to provide an overview of prediction errors and the proportion of variance explained [27][28][29].

2.5.1. Mean Squared Error (MSE)

$$\mathrm{MSE} = \frac{1}{n}\sum_{i=1}^{n}(y_i - \hat{y}_i)^2 \tag{5}$$

MSE serves as the optimization objective function during model training and quantifies the average squared prediction error across all OHLC components [27].

2.5.2. Root Mean Squared Error (RMSE)

$$\mathrm{RMSE} = \sqrt{\frac{1}{n}\sum_{i=1}^{n}(y_i - \hat{y}_i)^2} \tag{6}$$

RMSE expresses prediction error in the normalized price scale, facilitating interpretation of forecast accuracy relative to the [0, 1] data range [29].

2.5.3. Mean Absolute Error (MAE)

$$\mathrm{MAE} = \frac{1}{n}\sum_{i=1}^{n}|y_i - \hat{y}_i| \tag{7}$$

MAE provides a robust measure of average forecast error for the 7-day multi-step prediction horizon, less sensitive to outliers than squared error metrics [29].

2.5.4. Coefficient of Determination (R^2)

$$R^2 = 1 - \frac{\sum_{i=1}^{n}(y_i - \hat{y}_i)^2}{\sum_{i=1}^{n}(y_i - \bar{y})^2} \tag{8}$$

R^2 quantifies the proportion of Bitcoin price variance explained by the model, evaluating the predictive contribution of whale sentiment features [28].

2.6. Feature Denormalization

The LSTM model generates forecasts exclusively for the four OHLC components. Although the Min-Max scaler was originally fitted on the full dataset, which included an additional *sentiment_score* column, the model output does not contain predictions for *sentiment_score*. To apply the inverse transformation, a temporary array matching the scaler's original column dimensions was created, with the first four columns assigned the normalized OHLC forecasts and the *sentiment_score* column set to zero. The array was then processed through the inverse transformation, and only the four OHLC columns were retained as the final forecast output in USD.

Jurnal Teknik Informatika (JUTIF)
P-ISSN: 2723-3863
E-ISSN: 2723-3871
Vol. 7, No. 3, June 2026, Page. 2131-2153
https://jutif.if.unsoed.ac.id
DOI: https://doi.org/10.52436/1.jutif.2026.7.3.5436

3. RESULT

3.1. Datasets

3.1.1. Whale Transaction Data

The whale transaction dataset comprises 2,069 large-scale Bitcoin transfers (≥500 BTC) spanning from April 20, 2024, 00:00:00 UTC to April 20, 2025, 00:00:00 UTC. The distribution of transactions by category is presented in Table 4.

Table 4. Distribution of Whale Transactions by Category

Category	Count	Percentage
Unknown to Unknown	942	45.5%
Exchange to Unknown	602	29.1%
Unknown to Exchange	356	17.2%
Exchange to Exchange	169	8.2%
Total	**2,069**	**100%**

Based on Table 4, transactions are classified into four categories based on exchange involvement. Unknown-to-unknown transfers constitute the largest category at 45.5% (942 transactions), representing movements between non-exchange entities. Exchange outflows (exchange-to-unknown) account for 29.1% (602 transactions), while exchange inflows (unknown-to-exchange) comprise 17.2% (356 transactions). Inter-exchange transfers represent 8.2% (169 transactions). The higher proportion of outflows compared to inflows (602 vs 356) indicates net withdrawal activity from exchanges during this period.

3.1.2. Historical Bitcoin Price Data

The collected Bitcoin price data resulted in 8,761 hourly observations for the training period (April 20, 2024 to April 20, 2025) and 168 hourly observations for the test period (April 20-27, 2025). Figure 2 depicts the daily aggregated price movements throughout the training period.

Figure 2. Daily OHLC Bitcoin Prices (April 2024 - April 2025)

As depicted in Figure 2, the training dataset exhibits substantial price volatility across the 12-month period, with Bitcoin prices ranging from an absolute low of $49,849.22 USD (August 5, 2024)

Vol. 7, No. 3, June 2026, Page. 2131-2153
https://jutif.if.unsoed.ac.id
DOI: https://doi.org/10.52436/1.jutif.2026.7.3.5436

to an absolute high of $108,272.50 USD (December 17, 2024). The period from May through September 2024 was characterized by market consolidation and the lowest price level, followed by a significant bullish trend in the fourth quarter that culminated in the December peak, after which the market entered a corrective downtrend through the first quarter of 2025 before establishing a new consolidation range toward the end of the observation period in April 2025.

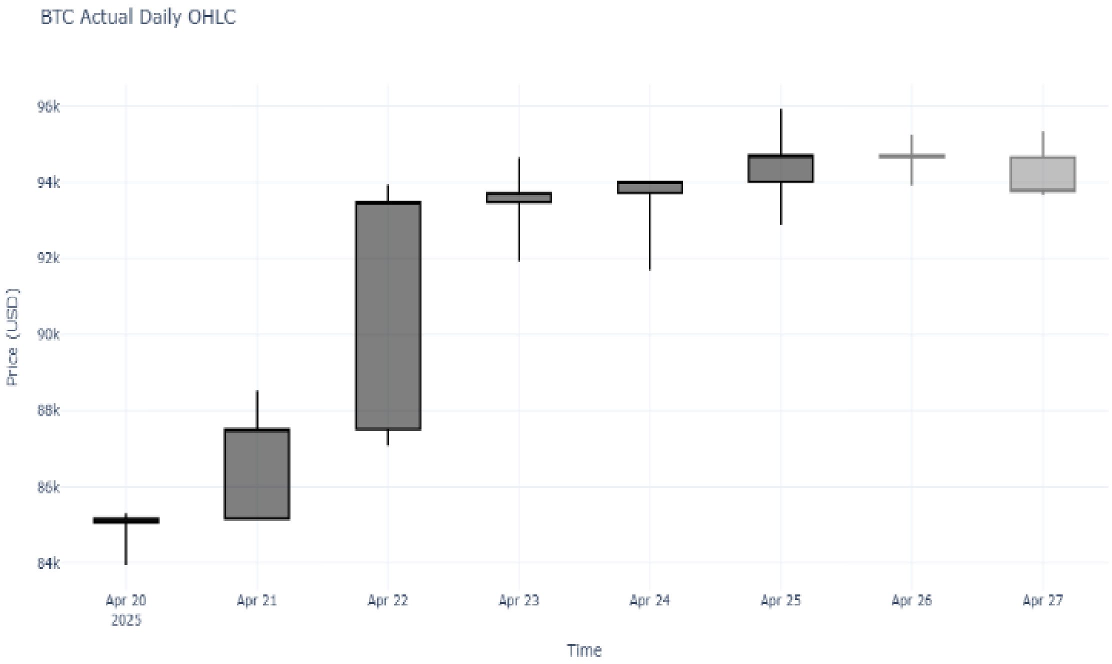

Figure 3. Actual Daily OHLC Bitcoin Prices (Test Period: April 20-27, 2025)

Figure 3 displays the actual daily OHLC Bitcoin prices during the test period from April 20 to April 27, 2025. The data show a price increase from an opening value of $85,061.54 on April 20 to a weekly closing value of $93,777.44 on April 27. The highest recorded price was $95,924.19 on April 25, while the lowest was $83,954.54 on April 20. The difference between the weekly high and low values indicates a total price range of approximately $11,970. This dataset covers a one-week period that includes both upward and range-bound movements, providing the reference for evaluating forecast results.

3.2. Transactions Scoring Results

3.2.1. Validation of Transaction-Level Sentiment Scores

Table 5 presents examples of computed whale transaction sentiment scores derived from the directional flow and magnitude of large Bitcoin transfers. Each transaction's scaled amount varies according to its BTC volume, while the sentiment score reflects the directional indicator. Exchange outflows, such as transfers from Binance to unknown wallets, resulted in positive sentiment values (e.g., 0.148411). In contrast, exchange inflows, such as transfers from unknown wallets to Kraken, produced negative sentiment scores (e.g., –0.191078). Transfers without exchange involvement, including unknown-to-unknown or exchange-to-exchange movements, maintained neutral scores of 0.000000, corresponding to zero directional influence on exchange liquidity.

Jurnal Teknik Informatika (JUTIF)
P-ISSN: 2723-3863
E-ISSN: 2723-3871

Vol. 7, No. 3, June 2026, Page. 2131-2153
https://jutif.if.unsoed.ac.id
DOI: https://doi.org/10.52436/1.jutif.2026.7.3.5436

Table 5. Example of Computed Whale Transaction Sentiment Scores

Date	Amount	USD Value	From	To	Category	Scaled_Amount	Sentiment_Score
2024-04-22 17:08:36	2000.0	132666651.0	unknown wallet	unknown wallet	unknown_to_unknown	0.302646	0.000000
2024-04-23 09:21:43	987.0	65379389.0	#Binance	unknown wallet	exchange_to_unknown	0.148411	0.148411
2024-04-26 14:22:02	1200.0	77563693.0	unknown wallet	#Kraken	unknown_to_exchange	0.191078	-0.191078
2024-05-16 20:46:06	979.0	61683724.0	Coinbase Institutional	#Coinbase	exchange_to_exchange	0.146635	0.000000

3.2.2. Longitudinal Analysis of Cumulative Whale Sentiment

Figure 4. Cumulative Whale Sentiment Score Over Time

Figure 4 presents the cumulative whale sentiment score over the 12-month period from April 2024 to April 2025, showing a gradual and consistent upward trajectory from near zero at the beginning of the observation window to a total value of 27.3547 by April 18, 2025. The sentiment values, derived from hourly-aggregated whale transaction data where positive scores correspond to exchange outflows and negative scores represent exchange inflows, demonstrate that positive sentiment events had a higher overall magnitude than negative ones throughout the year. This cumulative increase indicates the relative predominance of large Bitcoin transfers moving away from exchanges compared to those entering them, representing the net directional balance of whale transactions during the one-year period following the April 2024 halving event.

Vol. 7, No. 3, June 2026, Page. 2131-2153
https://jutif.if.unsoed.ac.id
DOI: https://doi.org/10.52436/1.jutif.2026.7.3.5436

3.2.3. Distributional Properties of Cumulative Sentiment Scores

Figure 5 presents the frequency distribution of cumulative whale sentiment scores across 8,761 hourly observations derived from 2,069 whale transaction entries. The distribution exhibits a multi-modal pattern with the highest concentration occurring in the 5 to 9 range (exceeding 1,000 observations), followed by additional peaks at 0 to 2 (approximately 500 observations), 14 to 16 (approximately 500 observations), and 18 to 20 (approximately 600 observations), with lower frequencies observed above 20. The distribution shows a median of 10.3935 (black dashed line) and a mean of 11.5066 (blue dashed line), with sentiment scores ranging from –1.1279 (May 2, 2024, 15:00:00) to 27.3547 (April 18, 2025, 02:00:00), where the mean's rightward shift relative to the median indicates positive skewness in the cumulative sentiment trajectory.

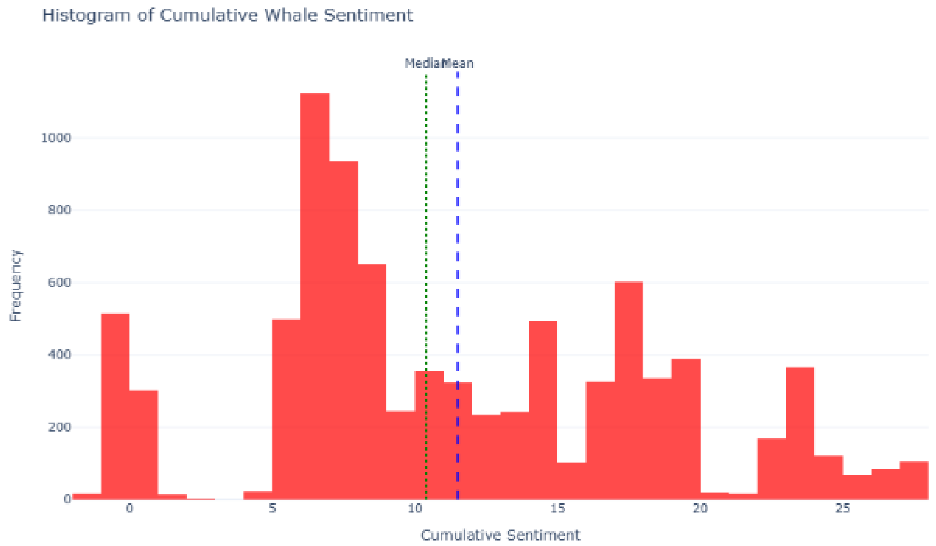

Figure 5. Distribution of Cumulative Whale Sentiment Scores

3.2.4. Correlation of BTC Price and Whale Sentiment

Figure 6. BTC Close Price vs Cumulative Whale Score

Figure 6 presents the temporal relationship between Bitcoin closing prices (blue line, left y-axis) and cumulative whale sentiment scores (red line, right y-axis) over the training period from May 2024

Vol. 7, No. 3, June 2026, Page. 2131-2153
https://jutif.if.unsoed.ac.id
DOI: https://doi.org/10.52436/1.jutif.2026.7.3.5436

to April 2025. Bitcoin closing prices ranged from a minimum of 49,849.22 USD (August 5, 2024) to a maximum of 108,272.5 USD (December 17, 2024), while cumulative whale sentiment scores ranged from –1.1279 (May 2, 2024) to 27.3547 (April 18, 2025). The temporal patterns reveal several phases: from May to August 2024, prices declined to their minimum while sentiment scores gradually increased from near 0 to approximately 5; from August to December 2024, prices surged to their maximum as sentiment scores rose from 5 to 15; following this peak, prices declined to approximately 75,000 USD by March 2025 while sentiment scores stabilized between 15 and 20; finally, from March to April 2025, prices recovered to approximately 108,000 USD as sentiment scores reached their maximum of 27.3547, indicating periods where both metrics exhibit aligned movements alongside segments of divergent patterns.

3.3. Data Preprocessing Results

3.3.1. Feature Integration

Table 6 displays four consecutive hourly observations from April 19, 2025, showing the original values before normalization. The Bitcoin price features (*open*, *high*, *low*, *close*) with values ranging from approximately 85,000 to 85,350 USD across the sample period. The *sentiment_score* feature shows a value of 0.0 for all four observations in this sample. Each row represents a single hourly time step containing all five features that were subsequently used for model training.

Table 6. Sample of Integrated Bitcoin OHLC and Whale Sentiment (Before Normalization)

Time	Open	High	Low	Close	Sentiment_Score
2025-04-19 20:00:00	85074.01	85250.30	85007.17	85185.92	0.0
2025-04-19 21:00:00	85185.92	85352.44	85176.61	85327.21	0.0
2025-04-19 22:00:00	85327.21	85339.17	85205.34	85239.99	0.0
2025-04-19 23:00:00	85239.99	85241.96	85056.87	85061.54	0.0

3.3.2. Feature Normalization

Table 7 presents sample data from the normalized dataset, showing four consecutive hourly observations from April 19, 2025. All feature values fall within the [0, 1] range as a result of the Min-Max normalization applied in the preprocessing phase. The normalized values represent the scaled positions of the original feature values within their respective minimum and maximum ranges across the entire dataset. Each normalized value reflects its proportional position between the dataset's minimum and maximum boundaries.

Table 7. Normalization Parameters and Sample Data

Time	Open	High	Low	Close	Sentiment_Score
2025-04-19 20:00:00	0.602924	0.583274	0.612515	0.604839	0.519398
2025-04-19 21:00:00	0.602924	0.585040	0.615413	0.607258	0.519398
2025-04-19 22:00:00	0.607258	0.584811	0.615905	0.605765	0.519398
2025-04-19 23:00:00	0.605765	0.583129	0.613365	0.602710	0.519398

P-ISSN: 2723-3863
https://jutif.if.unsoed.ac.id
E-ISSN: 2723-3871
DOI: https://doi.org/10.52436/1.jutif.2026.7.3.5436

3.4. LSTM Model Architecture

Table 8 presents the architecture summary of the LSTM model, detailing the layer configuration, output shapes, and parameter counts. The model consists of two LSTM layers with 128 and 64 units respectively, each followed by a dropout layer. The first LSTM layer produces an output shape of (None, 720, 128), containing 68,608 parameters. The second LSTM layer outputs a shape of (None, 64) with 49,408 parameters. The final dense layer transforms the output to (None, 672) with 43,680 parameters. The total number of trainable parameters in the model is 161,696, with no non-trainable parameters present.

Table 8. LSTM Model Architecture Summary

Layer	Output Shape	Param #
lstm (LSTM)	(None, 720, 128)	68,608
dropout (Dropout)	(None, 720, 128)	0
lstm_1 (LSTM)	(None, 64)	49,408
dropout_1 (Dropout)	(None, 64)	0
dense (Dense)	(None, 672)	43,680
Total params		161,696
Trainable params		161,696
Non-trainable params		0

3.5. Model Training Performance

Table 9 presents the training and validation loss values across 20 epochs. The training loss decreased continuously from 0.0704 in epoch 1 to 0.0039 in epoch 20. The most substantial reduction occurred between epoch 1 and epoch 2 (from 0.0704 to 0.0067), after which the training loss declined gradually, stabilizing around 0.0039 to 0.0040 from epoch 17 onwards. The training duration for each epoch ranged from 307 to 331 seconds, averaging approximately 313 seconds per epoch.

Table 9. Training and Validation Loss Over Epochs

Epoch	Training Loss	Validation Loss	Training Duration (s)
1	0.0704	0.0082	317
2	0.0067	0.0098	318
3	0.0057	0.0114	312
4	0.0055	0.0084	313
5	0.0050	0.0117	312
6	0.0048	0.0130	307
7	0.0045	0.0095	308
8	0.0045	0.0152	320
9	0.0044	0.0045	308
10	0.0045	0.0127	309
11	0.0041	0.0126	331
12	0.0042	0.0108	310
13	0.0042	0.0130	308
14	0.0040	0.0138	310
15	0.0040	0.0130	308
16	0.0040	0.0111	324
17	0.0039	0.0105	307
18	0.0040	0.0132	325
19	0.0039	0.0177	307
20	0.0039	0.0144	322

P-ISSN: 2723-3863 https://jutif.if.unsoed.ac.id
E-ISSN: 2723-3871 DOI: https://doi.org/10.52436/1.jutif.2026.7.3.5436

The validation loss reached its minimum value of 0.0045 at epoch 9. Following this point, the validation loss exhibited fluctuations and an upward trend, increasing to 0.0144 by epoch 20, with a peak of 0.0177 at epoch 19. This divergence between the consistently decreasing training loss and the rising validation loss after epoch 9 indicates overfitting [30]. The model was trained without early stopping mechanisms, resulting in the final epoch weights being saved for subsequent evaluation. This training configuration represents a limitation of the study, as the model may have achieved better generalization if training had been halted at epoch 9 when validation loss was minimized. The observed overfitting behaviour is considered when interpreting test results, particularly regarding the model's systematic underestimation of prices during periods of high volatility.

Table 10. Model Performance Metrics on Training Data

Metric	Value	Interpretation
MSE	0.004699	Mean squared prediction error
RMSE	0.068550	Root mean squared error on normalized scale
MAE	0.049824	Mean absolute error on normalized scale
R^2	0.9386	Proportion of variance explained

Table 10 presents the model's performance metrics evaluated on the training dataset. The model achieves an MSE of 0.004699, RMSE of 0.068550, and MAE of 0.049824 on the normalized scale (0-1 range). The RMSE and MAE correspond to approximately 6.86% and 4.98% of the normalized range respectively, indicating relatively small average prediction errors. The MAE/RMSE ratio of 0.727 suggests that prediction errors follow a relatively consistent distribution, with occasional larger deviations contributing disproportionately to the squared error metric. This pattern is characteristic of financial time series forecasting, where extreme market movements can generate outlier predictions that inflate RMSE relative to MAE.

The coefficient of determination (R^2) of 0.9386 indicates that the LSTM architecture captures 93.86% of the variance in Bitcoin OHLC price movements within the training period. The remaining 6.14% of unexplained variance likely reflects inherent market stochasticity, external macroeconomic events, and behavioural factors not represented in the input features. However, these training metrics must be interpreted with caution given the observed overfitting pattern documented in Table 9, where validation loss diverged from training loss after epoch 9. Training performance may therefore overestimate the model's generalization capability, and true predictive power is assessed through out-of-sample forecasting on the held-out test period spanning April 20-27, 2025.

3.6. Denormalized Forecast Output

Table 11 presents a sample of the denormalized forecast output, showing the first five hourly predictions from April 20, 2025, 01:00:00 to April 20, 2025, 05:00:00 in original USD price scale.

Table 11. Sample Denormalized Forecast

Time	Open	High	Low	Close
2025-04-20 01:00:00	87330.762603	87796.948286	87002.385921	87417.865345
2025-04-20 02:00:00	87406.049904	87820.016543	87021.444339	87439.452115
2025-04-20 03:00:00	87427.883918	87812.157141	87023.165520	87435.377825
2025-04-20 04:00:00	87393.001731	88005.896052	87155.595400	87603.865373

Jurnal Teknik Informatika (JUTIF) Vol. 7, No. 3, June 2026, Page. 2131-2153
P-ISSN: 2723-3863 https://jutif.if.unsoed.ac.id
E-ISSN: 2723-3871 DOI: https://doi.org/10.52436/1.jutif.2026.7.3.5436

Based on Table 11, the inverse transformation successfully restored the forecast values to the original USD price scale. The denormalized predictions show OHLC values ranging from approximately 87,002.39 USD (low) to 88,007.55 USD (high) during the initial five hours of the forecast period. The reconstructed values maintain proper OHLC relationships, with high values consistently exceeding open and close values, and low values remaining below them. This denormalization enables direct comparison between forecasted prices and actual market prices recorded during the test period, facilitating practical interpretation of model performance in absolute USD terms rather than normalized scale.

3.7. Forecast Results and Comparison with Actual Prices

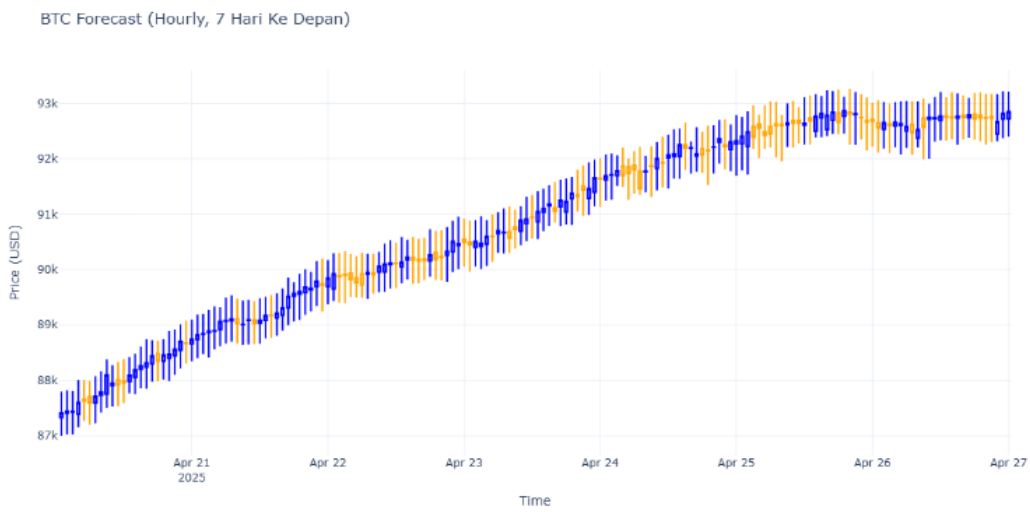

Figure 7. Bitcoin Price Forecast (Hourly, 7-Day Ahead)

Figure 8. Bitcoin Actual Price (Hourly OHLC)

The trained LSTM model produced 7-day (168-hour) Bitcoin price forecasts from April 20 to 27, 2025, which were compared with actual prices for performance evaluation. Figure 7 presents the hourly forecast results displayed as candlestick charts. The forecast shows a general upward trend throughout the 7-day period, with predicted prices starting at approximately 87,330 USD on April 20 and gradually increasing to approximately 92,850 USD by April 27. The forecast exhibits relatively stable progression

Vol. 7, No. 3, June 2026, Page. 2131-2153
https://jutif.if.unsoed.ac.id
DOI: https://doi.org/10.52436/1.jutif.2026.7.3.5436

with moderate intraday fluctuations. The predicted high-low ranges remain relatively consistent across the forecast period, with the highest forecasted value reaching 93,256.14 USD and the lowest at 87,002.39 USD.

Figure 8 presents the actual Bitcoin prices recorded during the forecast period as a continuous candlestick chart. The period begins at approximately 85,144 USD on April 20, showing initial stability around 84,000-86,000 USD during Day 1 (range: 83,954.54-86,992.00 USD). Day 2 (April 21) exhibits moderate upward movement within the range of 86,385.92-88,526.30 USD. Day 3 (April 22) displays the most substantial price action, with a dramatic surge from approximately 87,500 USD to above 93,000 USD (range: 87,514.56-93,937.07 USD). Days 4-7 maintain elevated price levels with Day 4 (April 23) showing 91,943.03-94,656.65 USD, Day 5 (April 24) at 91,693.21-94,052.97 USD, Day 6 (April 25) reaching the highest point at 92,883.11-95,924.19 USD, and Day 7 (April 26) maintaining 93,916.48-95,258.03 USD.

3.7.1. Daily Forecast Performance

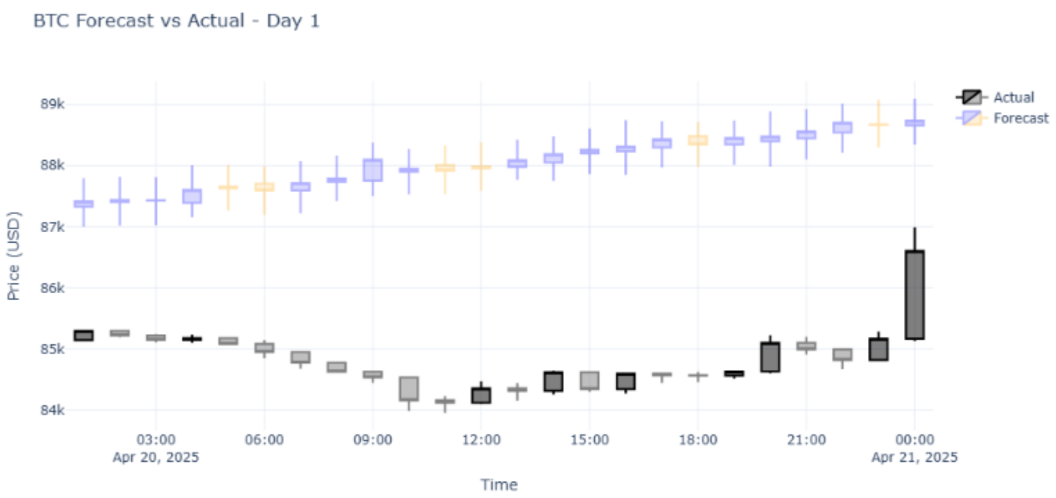

Figure 9. Day 1 Forecast vs Actual (April 20, 2025)

Figure 9 presents the hourly comparison for Day 1, with actual prices shown in black candlesticks and forecast prices in blue and orange candlesticks. The actual prices (lower section) range from 83,954.54 to 86,992.00 USD, displaying relatively stable movement with a notable upward spike near the end of the day reaching approximately 87,000 USD. The forecast prices (upper section) range from 87,002.39 to 89,093.77 USD, showing a gradual upward trend throughout the day. The forecast consistently overestimated actual prices by approximately 2,000-3,000 USD. Day 1 recorded average MAE values of 3,246.85 USD (open), 3,482.27 USD (high), 3,036.06 USD (low), and 3,250.70 USD (close).

Figure 10 displays the Day 2 comparison. The actual prices (lower section) range from 86,385.92 to 88,526.30 USD, starting around 86,600 USD and ending near 87,500 USD with a notable spike to approximately 88,500 USD during mid-day. The forecast prices (upper section) range from 88,400.50 to 90,201.28 USD, maintaining a steady upward progression. The forecast overestimated actual prices, though the gap narrowed compared to Day 1. Day 2 recorded average MAE values of 1,890.16 USD (open), 1,996.52 USD (high), 1,774.87 USD (low), and 1,891.87 USD (close), representing improved forecast accuracy.

Vol. 7, No. 3, June 2026, Page. 2131-2153
https://jutif.if.unsoed.ac.id
DOI: https://doi.org/10.52436/1.jutif.2026.7.3.5436

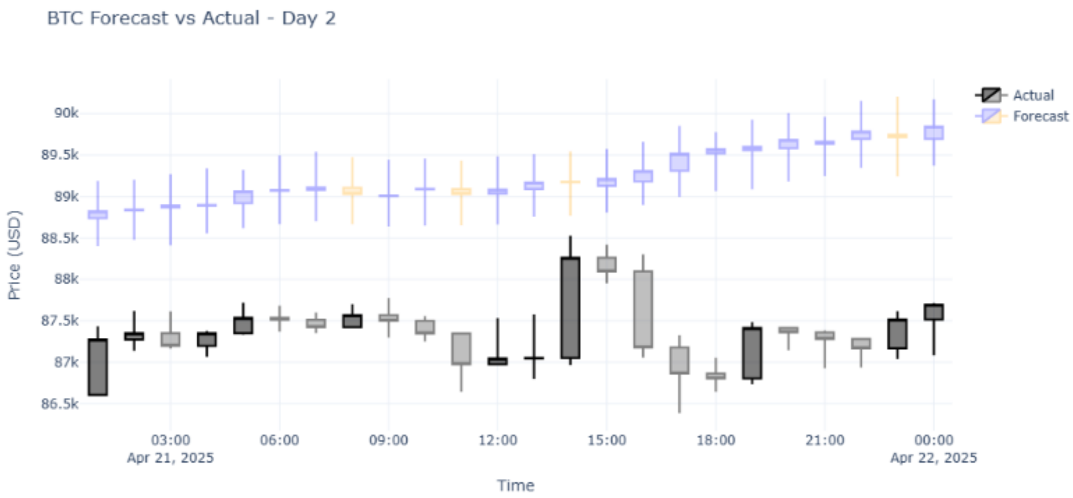

Figure 10. Day 2 Forecast vs Actual (April 21, 2025)

Figure 11. Day 3 Forecast vs Actual (April 22, 2025)

Figure 11 shows the Day 3 comparison, which exhibits the most dramatic divergence in behavior. The actual prices (lower section) range from 87,514.56 to 93,937.07 USD, beginning around 87,700 USD and ending above 93,400 USD, with a sharp upward movement starting around 12:00 that continues through the end of the day. The forecast prices (upper section) range from 89,394.88 to 90,951.09 USD, showing gradual linear progression. Despite the substantial actual price surge, Day 3 recorded the lowest average MAE values: 1,477.92 USD (open), 1,600.21 USD (high), 1,417.35 USD (low), and 1,495.47 USD (close), as the forecast values began closer to actual prices before the surge.

Figure 12 presents the Day 4 comparison. The actual prices (upper section) range from 91,943.03 to 94,656.65 USD, starting around 92,900 USD and showing volatility throughout the day with a notable dip to approximately 92,000 USD during mid-day before recovering. The forecast prices (lower section) range from 89,962.56 to 92,009.65 USD, continuing the gradual upward trend. The forecast significantly underestimated the new elevated price level. Day 4 recorded increased MAE values of 2,597.23 USD (open), 2,477.80 USD (high), 2,646.84 USD (low), and 2,562.06 USD (close).

Vol. 7, No. 3, June 2026, Page. 2131-2153
https://jutif.if.unsoed.ac.id
DOI: https://doi.org/10.52436/1.jutif.2026.7.3.5436

Figure 12. Day 4 Forecast vs Actual (April 23, 2025)

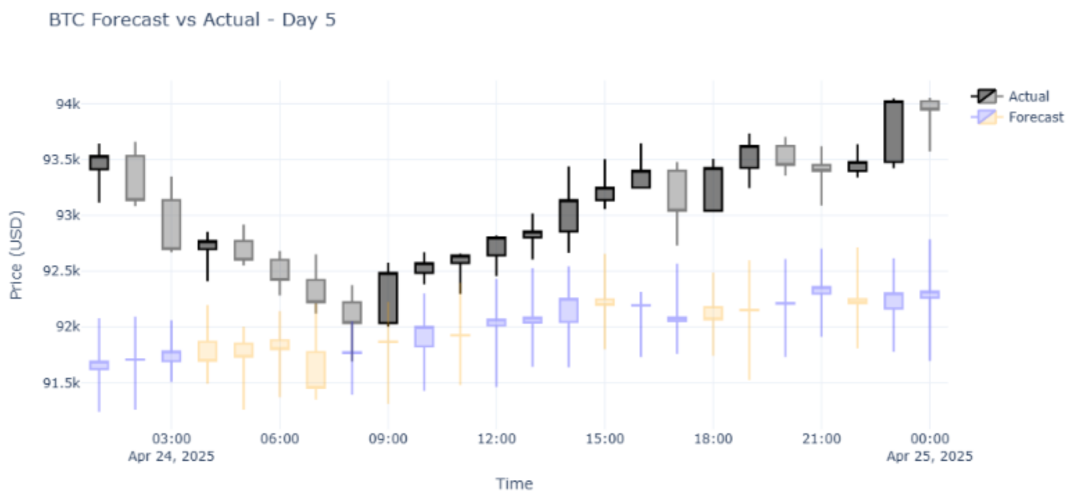

Figure 13. Day 5 Forecast vs Actual (April 24, 2025)

Figure 13 displays the Day 5 comparison. The actual prices (upper section) range from 91,693.21 to 94,052.97 USD, beginning around 93,400 USD, declining to approximately 92,000 USD during the first half of the day, then recovering to around 94,000 USD by day's end. The forecast prices (lower section) range from 91,241.12 to 92,787.08 USD, maintaining steady progression. Day 5 achieved the best forecast performance with average MAE values of 1,020.98 USD (open), 871.72 USD (high), 1,212.50 USD (low), and 1,041.82 USD (close), as the forecast values aligned more closely with the lower portion of actual price movements.

Figure 14 shows the Day 6 comparison. The actual prices (upper section) range from 92,883.11 to 95,924.19 USD, starting around 93,700 USD and reaching a peak of approximately 95,900 USD during mid-day before stabilizing around 94,700 USD. The forecast prices (lower section) range from 91,713.82 to 93,256.14 USD, continuing gradual upward movement. The gap between forecast and actual prices widened as actual prices reached their highest levels. Day 6 recorded MAE values of 1,657.23 USD (open), 1,608.44 USD (high), 1,826.82 USD (low), and 1,682.61 USD (close).

Jurnal Teknik Informatika (JUTIF)
P-ISSN: 2723-3863
E-ISSN: 2723-3871
Vol. 7, No. 3, June 2026, Page. 2131-2153
https://jutif.if.unsoed.ac.id
DOI: https://doi.org/10.52436/1.jutif.2026.7.3.5436

Figure 14. Day 6 Forecast vs Actual (April 25, 2025)

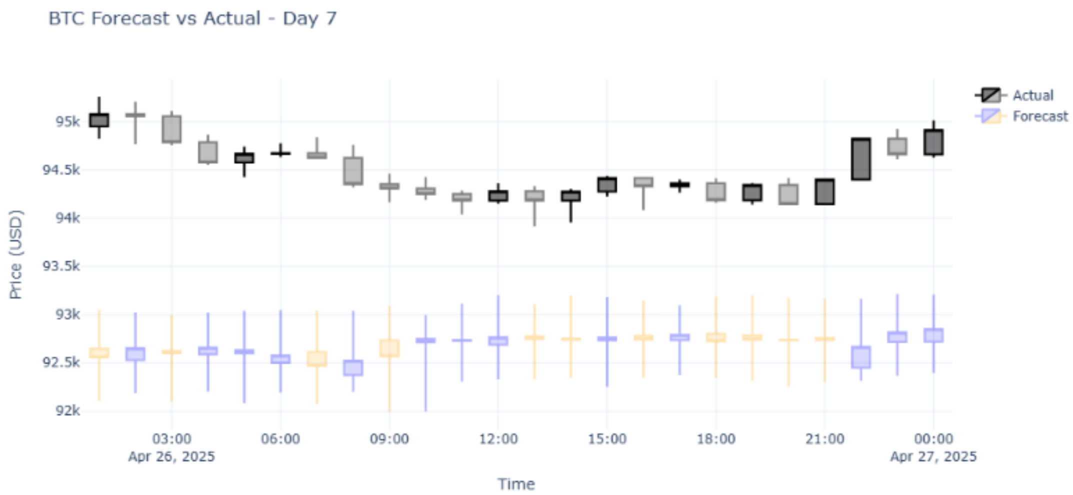

Figure 15. Day 7 Forecast vs Actual (April 26, 2025)

Figure 15 presents the Day 7 comparison. The actual prices (upper section) range from 93,916.48 to 95,258.03 USD, showing relatively stable movement around 94,000-95,000 USD with minor fluctuations throughout the day. The forecast prices (lower section) range from 91,991.91 to 93,216.67 USD, maintaining consistent upward progression. The forecast continued to underestimate the elevated price levels. Day 7 recorded MAE values of 1,825.85 USD (open), 1,526.62 USD (high), 2,100.21 USD (low), and 1,806.00 USD (close).

The comprehensive comparison reveals that the LSTM model's forecast captured the directional trend (upward movement) but failed to anticipate both the magnitude and timing of the sharp price increase that occurred on Day 3. The forecast demonstrated best performance on Day 5 with MAE values below 1,300 USD for all OHLC components, while the highest errors occurred on Days 1 and 4 with MAE values exceeding 2,400 USD. The persistent underestimation of prices from Day 4 onwards indicates the model's limitation in adapting to sudden market regime changes reflected in the actual price data.

Vol. 7, No. 3, June 2026, Page. 2131-2153
https://jutif.if.unsoed.ac.id
DOI: https://doi.org/10.52436/1.jutif.2026.7.3.5436

4. DISCUSSIONS

4.1. Forecast Performance

The LSTM model exhibited variable accuracy over the 7-day horizon, with MAE ranging from 871.72 USD to 3,482.27 USD across OHLC components. Optimal performance occurred on Day 5 (April 24) with MAE below 1,300 USD, while Day 1 (April 20) recorded the highest errors exceeding 3,000 USD. Although the model systematically underestimated price increases from Day 4 onward and failed to capture abrupt surges like Day 3 (April 22, +6,000 USD), it consistently identified the overall market direction, successfully indicating general bullish trends over the period (≈87,330 USD → 92,850 USD). This suggests that while precise price forecasting remains challenging, the model effectively captures trend signals.

4.2. Whale Sentiment as a Predictive Feature

Cumulative whale sentiment increased from near zero (May 2024) to 27.35 (April 2025), reflecting net exchange outflows. While sentiment partially aligned with price trends—accumulation during May–August 2024 decline and August–December 2024 rally—the relationship is non-linear and time-lagged. The model did not predict short-term surges like Day 3, though whale sentiment helped capture directional trends, reinforcing its value for identifying bullish or bearish periods.

The cumulative nature of the whale sentiment score, while effective for capturing long-term accumulation or distribution trends, inherently smooths short-term signals. Additionally, the threshold of 500 BTC for whale transaction identification may not capture patterns from coordinated smaller transactions or increased transaction frequency that could precede rapid price movements. These feature design choices prioritize medium-term trend signals over short-term volatility detection, aligning with the model's demonstrated strength in directional forecasting.

4.3. Model Architecture and Training Considerations

The LSTM architecture (two layers: 128 and 64 units; 161,696 parameters) exhibited overfitting, shown by divergence between training loss (0.0044 → 0.0039) and validation loss (0.0045 → 0.0144) post-epoch 9. The architecture compresses 720 hours of historical data into a fixed-length representation, which means that recent whale activity represents only a small fraction of the temporal context, potentially diluting immediate pre-surge signals. This input window design prioritizes medium-term trend context over short-term reactivity, contributing to the model's inability to anticipate abrupt intraday movements like the Day 3 surge. Alternative architectures, such as encoder-decoder or attention-based models, could better handle extended temporal dependencies and potentially improve short-term price prediction, though trend detection remains feasible with the current setup.

4.4. Comparison with Previous Research

Consistent with prior LSTM studies, forecast accuracy declines over longer horizons. Incorporation of on-chain metrics, particularly whale activity, can provide insight into market direction even if short-term price precision is limited. Overfitting and limited dataset exposure are common challenges in financial time series modeling, reinforcing that LSTM models are generally more reliable for trend identification than exact price forecasting prices.

4.5. Limitations and Practical Implications

Several limitations affect interpretation. The 7-day forecast horizon exceeds typical LSTM reliability for precise cryptocurrency pricing, with accuracy declining beyond 2–3 days. Whale sentiment, based on cumulative scores, may overlook nuanced market activity, and focus on >500 BTC

Vol. 7, No. 3, June 2026, Page. 2131-2153
https://jutif.if.unsoed.ac.id
DOI: https://doi.org/10.52436/1.jutif.2026.7.3.5436

transactions may miss smaller but influential movements. The training period (April 2024–April 2025) represents a post-halving phase, limiting generalizability.

Despite these constraints, the model reliably captures general market trends. Forecasts are more suitable for identifying bullish or bearish conditions rather than exact price points. Systematic underestimation beyond Day 4 highlights limitations in short-term precision but does not diminish the utility for trend-based strategic positioning. Integration of whale sentiment demonstrates a methodological framework for combining on-chain metrics with neural networks, which could be enhanced with refined feature engineering or alternative architectures.

4.6. Methodological Contribution to Computational Finance

This study advances cryptocurrency forecasting methodologies by demonstrating the integration of blockchain-native behavioural indicators into LSTM architectures. The directional whale sentiment scoring mechanism represents a novel operationalization of on-chain transaction data that quantifies institutional behaviour beyond binary whale detection approaches. By empirically evaluating whether directionally-weighted large-holder activity enhances predictive accuracy, this research establishes a replicable framework for incorporating blockchain-specific features into time series forecasting models. The findings clarify the distinction between directional trend identification and precise point prediction in cryptocurrency markets, contributing theoretical understanding of feature engineering constraints and architectural limitations in deep learning applications for volatile financial assets. Furthermore, the explicit documentation of overfitting dynamics advances methodological transparency in cryptocurrency forecasting research, informing both model selection decisions and realistic performance expectations for practitioners deploying neural networks in decentralized market contexts.

4.7. Implications for Future Research

The findings suggest several directions for future research. Improving feature engineering for whale transaction data, such as temporal weighting of recent activity, differentiating exchanges by market role, categorizing transactions by participant type (e.g., institutional investors, national entities, market makers), or incorporating transaction velocity metrics, could enhance predictive power. Alternative neural network architectures, including transformer-based models with attention mechanisms, may better capture complex temporal dependencies between whale activity and price movements. Ensemble approaches combining multiple LSTM models trained on different periods or feature sets could increase robustness to regime shifts, such as the Day 3 surge observed in the test period. Expanding the training dataset to cover multiple Bitcoin halving cycles would expose the model to diverse market conditions, while incorporating additional on-chain metrics such as active addresses, transaction volumes, miner behaviour, or network hash rate could improve forecast accuracy. Investigating optimal forecast horizons for specific trading strategies, for example 24-hour for day trading, 72-hour for swing trading, or 7-day for position adjustment, may identify time scales with higher reliability. Developing uncertainty quantification methods, such as confidence intervals around point forecasts, would enhance practical decision-making by providing measures of prediction reliability.

5. CONCLUSION

This study demonstrates that integrating whale transaction sentiment with historical Bitcoin OHLC data in an LSTM framework can effectively capture short-term directional trends, yet it remains limited in predicting precise price levels over a seven-day horizon. While the model successfully identified the overall upward trajectory during the test period, systematic underestimation and the inability to anticipate abrupt intraday surges highlight the constraints of cumulative sentiment aggregation and fixed 720-hour input windows. The findings suggest that whale transaction directionality serves as a useful indicator for trend recognition rather than exact price forecasting. From

Vol. 7, No. 3, June 2026, Page. 2131-2153
https://jutif.if.unsoed.ac.id
DOI: https://doi.org/10.52436/1.jutif.2026.7.3.5436

a practical perspective, the model's directional forecasting capability makes it more suitable for medium-term trading strategies, such as swing trading or position adjustment decisions, rather than high-frequency trading where precise entry and exit price points are critical. Traders could leverage the model's trend signals to identify favorable bullish or bearish conditions over multi-day periods, while acknowledging that forecasts should be interpreted as directional guidance rather than definitive price targets. Future improvements may involve incorporating temporal weighting of recent whale activity, exploring transformer-based architectures with attention mechanisms, leveraging ensemble modeling across different time periods, and integrating additional on-chain metrics to enhance granularity and forecast accuracy.

REFERENCES

[1] S. Nakamoto, "Bitcoin: A Peer-to-Peer Electronic Cash System." [Online]. Available: www.bitcoin.org

[2] A. D. Gbadebo, A. O. Adekunle, W. Adedokun, A. O. A. Lukman, and J. Akande, "BTC price volatility: Fundamentals versus information," *Cogent Business and Management*, vol. 8, no. 1, 2021, doi: 10.1080/23311975.2021.1984624.

[3] J. Chen, "Analysis of Bitcoin Price Prediction Using Machine Learning," *Journal of Risk and Financial Management*, vol. 16, no. 1, Jan. 2023, doi: 10.3390/jrfm16010051.

[4] D. G. Baur and T. Dimpfl, "The volatility of Bitcoin and its role as a medium of exchange and a store of value," *Empir Econ*, vol. 61, no. 5, pp. 2663–2683, Nov. 2021, doi: 10.1007/s00181-020-01990-5.

[5] M. Nedved and L. Kristoufek, "Safe havens for Bitcoin," *Financ Res Lett*, vol. 51, Jan. 2023, doi: 10.1016/j.frl.2022.103436.

[6] A. Liu, H. Jahanshahloo, J. Chen, and A. Eshraghi, "Trading patterns in the bitcoin market," *European Journal of Finance*, 2023, doi: 10.1080/1351847X.2023.2241883.

[7] Z. Ye, Y. Wu, H. Chen, Y. Pan, and Q. Jiang, "A Stacking Ensemble Deep Learning Model for Bitcoin Price Prediction Using Twitter Comments on Bitcoin," *Mathematics*, vol. 10, no. 8, Apr. 2022, doi: 10.3390/math10081307.

[8] H. A. Aalborg, P. Molnár, and J. E. de Vries, "What can explain the price, volatility and trading volume of Bitcoin?," *Financ Res Lett*, vol. 29, pp. 255–265, Jun. 2019, doi: 10.1016/J.FRL.2018.08.010.

[9] A. Chernoff and J. Jagtiani, "Beneath the Crypto Currents: The Hidden Effect of Crypto 'Whales,'" Federal Reserve Bank of Philadelphia, Philadelphia, PA, Jul. 2024. doi: 10.21799/frbp.wp.2024.14.

[10] J. M. Griffin and A. Shams, "Is Bitcoin Really Untethered?," *Journal of Finance*, vol. 75, no. 4, pp. 1913–1964, Aug. 2020, doi: 10.1111/jofi.12903.

[11] V. Derbentsev, A. Matviychuk, and V. N. Soloviev, "Forecasting of Cryptocurrency Prices Using Machine Learning," in *Advanced Studies of Financial Technologies and Cryptocurrency Markets*, Springer Singapore, 2020, pp. 211–231. doi: 10.1007/978-981-15-4498-9_12.

[12] I. E. Livieris, E. Pintelas, S. Stavroyiannis, and P. Pintelas, "Ensemble Deep learning models for forecasting cryptocurrency time-series," *Algorithms*, vol. 13, no. 5, May 2020, doi: 10.3390/A13050121.

[13] P. S. T. P. Purnama, "Optimizing Bitcoin Price Prediction with LSTM: A Comprehensive Study on Feature Engineering and the April 2024 Halving Impact," *Elinvo (Electronics, Informatics, and Vocational Education)*, vol. 9, no. 1, pp. 165–177, Oct. 2024, doi: 10.21831/elinvo.v9i1.72518.

[14] Y. Li and W. Dai, "Bitcoin price forecasting method based on CNN-LSTM hybrid neural network model," *The Journal of Engineering*, vol. 2020, no. 13, pp. 344–347, Jul. 2020, doi: 10.1049/joe.2019.1203.

[15] L. Ante and I. Fiedler, "Market reaction to large transfers on the Bitcoin blockchain - Do size and motive matter?," *Financ Res Lett*, vol. 39, p. 101619, Mar. 2021, doi: 10.1016/J.FRL.2020.101619.

[16] V. Chutipat, R. Kasemrat, T. Kraiwanit, and I. Phaksipaeng, "SELECTION OF CRYPTOCURRENCY EXCHANGE PLATFORMS IN A DEVELOPING ECONOMY," *Corporate and Business Strategy Review*, vol. 4, no. 2 Special Issue, pp. 344–350, 2023, doi: 10.22495/cbsrv4i2siart14.

[17] F. Fang *et al.*, "Cryptocurrency trading: a comprehensive survey," Dec. 01, 2022, *Springer Science and Business Media Deutschland GmbH*. doi: 10.1186/s40854-021-00321-6.

[18] M. Anas, S. J. H. Shahzad, and L. Yarovaya, "The use of high-frequency data in cryptocurrency research: a meta-review of literature with bibliometric analysis," Dec. 01, 2024, *Springer Science and Business Media Deutschland GmbH*. doi: 10.1186/s40854-023-00595-y.

[19] P. Jaquart, D. Dann, and C. Weinhardt, "Short-term bitcoin market prediction via machine learning," *Journal of Finance and Data Science*, vol. 7, pp. 45–66, Nov. 2021, doi: 10.1016/j.jfds.2021.03.001.

[20] I. E. Livieris, N. Kiriakidou, S. Stavroyiannis, and P. Pintelas, "An Advanced CNN-LSTM Model for Cryptocurrency Forecasting," 2021, doi: 10.3390/electronics.

[21] Z. Chen, C. Li, and W. Sun, "Bitcoin price prediction using machine learning: An approach to sample dimension engineering," *J Comput Appl Math*, vol. 365, Feb. 2020, doi: 10.1016/j.cam.2019.112395.

[22] L. Kristoufek, "Grandpa, Grandpa, Tell Me the One About Bitcoin Being a Safe Haven: New Evidence From the COVID-19 Pandemic," *Front Phys*, vol. 8, Jul. 2020, doi: 10.3389/fphy.2020.00296.

[23] H. Sebastião and P. Godinho, "Forecasting and trading cryptocurrencies with machine learning under changing market conditions," *Financial Innovation*, vol. 7, no. 1, Dec. 2021, doi: 10.1186/s40854-020-00217-x.

[24] Y. S. Kim, M. K. Kim, N. Fu, J. Liu, J. Wang, and J. Srebric, "Investigating the impact of data normalization methods on predicting electricity consumption in a building using different artificial neural network models," *Sustain Cities Soc*, vol. 118, Jan. 2025, doi: 10.1016/j.scs.2024.105570.

[25] Z. Li, H. Yu, J. Xu, J. Liu, and Y. Mo, "Stock Market Analysis and Prediction Using LSTM: A Case Study on Technology Stocks," *Innovations in Applied Engineering and Technology*, pp. 1–6, Nov. 2023, doi: 10.62836/iaet.v2i1.162.

[26] S. S. de Souza and J. E. Silva, "Application of LSTM recurrent neural networks for bitcoin price prediction," *REVISTA DELOS*, vol. 17, no. 61, p. e2602, Nov. 2024, doi: 10.55905/rdelosv17.n61-062.

[27] S. Ahmed, S. U. Hassan, N. R. Aljohani, and R. Nawaz, "FLF-LSTM: A novel prediction system using Forex Loss Function," *Applied Soft Computing Journal*, vol. 97, Dec. 2020, doi: 10.1016/j.asoc.2020.106780.

[28] D. Chicco, M. J. Warrens, and G. Jurman, "The coefficient of determination R-squared is more informative than SMAPE, MAE, MAPE, MSE and RMSE in regression analysis evaluation," *PeerJ Comput Sci*, vol. 7, pp. 1–24, 2021, doi: 10.7717/PEERJ-CS.623.

[29] T. O. Hodson, "Root-mean-square error (RMSE) or mean absolute error (MAE): when to use them or not," Jul. 19, 2022, *Copernicus GmbH*. doi: 10.5194/gmd-15-5481-2022.

[30] H. Li, G. K. Rajbahadur, D. Lin, C.-P. Bezemer, Z. Ming, and Jiang, "Keeping Deep Learning Models in Check: A History-Based Approach to Mitigate Overfitting," Jan. 2024, doi: 10.1109/ACCESS.2024.3402543.